# La- and La-/Ce-Doped $BaF_2$ Crystals for Future HEP Experiments at the Energy and Intensity Frontiers Part II

Fan Yang, *Member, IEEE*, Junfeng Chen, *Member, IEEE*, Liyuan Zhang, *Member, IEEE*, Chen Hu, *Member, IEEE*, and Ren-Yuan Zhu, *Senior Member, IEEE*

***Abstract*— In addition to La-doped barium fluoride ($BaF_2$) crystals, La/Ce co-doped $BaF_2$ crystals were also investigated at the California Institute of Technology, Pasadena, CA, USA. Strong cerium-induced emissions peaked at 305 and 320 nm with a decay time of 25 ns were observed, in addition to the fast and slow scintillation at 220 and 300 nm, respectively. The La/Ce co-doping was also found effective in suppressing the slow component in $BaF_2$. Compared to La-doped crystals, the La/Ce co-doped crystals have a better light output in both 50- and 2500-ns gate. The fast/slow ratio of La/Ce co-doped crystal was found to be about 1/1, similar to La-doping, which is also considered not sufficient for pile-up suppression. A 20-cm-long La/Ce co-doped $BaF_2$ crystal shows also excellent optical quality and light response uniformity.**

***Index Terms*— Barium fluoride ($BaF_2$), rare earth doping, slow scintillation component suppression.**

## I. Introduction

THE slow component suppression in barium fluoride ($BaF_2$) crystals is crucial for applications of this ultra-fast inorganic scintillator in the next-generation calorimeters required to take an unprecedented high event rate expected in future high-energy physics (HEP) experiments [1]–[5]. In the Part I of this paper, our investigation on La-doped $BaF_2$ crystals is reported. The La-doping suppresses the slow component and improves the fast/slow (F/S) ratio of crystal's light output from 1/5 to 1/1, which is considered not sufficient for pile-up suppression. In the Part II of this paper, we report our investigations carried out at the HEP Crystal Lab California Institute of Technology, Pasadena, CA, USA (Caltech) on La/Ce co-doped $BaF_2$ crystals grown at the Beijing Glass Research Institute (BGRI). An early result of this investigation was presented in the Nuclear Science Symposium 2016 Conference [6]. Ce-doping was also investigated by Visser *et al.* [7], Woody *et al.* [8], Dorenbos *et al.* [9], and Kurosawa *et al.* [10]. It was found to induce a strong UV absorption, which shifts the UV cutoff edge to longer than 300 nm, causing a serious self-absorption for the 220-nm fast component.

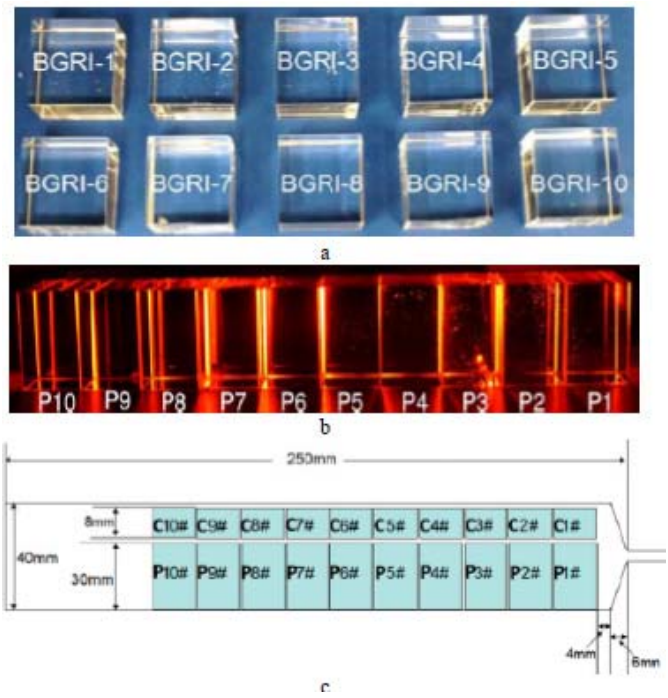


Fig. 1. (a) 10 La/Ce co-doped $BaF_2$ from BGRI. (b) Illuminated by a red LED. (c) Position of 20 samples in the La/Ce co-doped ingot.

## II. Lanthanum and Cerium co-Doped $BaF_2$ Crystals

Similar to La-doped samples from SIC, 10 $3 \times 3 \times 2$ $cm^3$ samples were cut from a La/Ce co-doped $BaF_2$ ingot grown at BGRI. Fig. 1(a) shows these samples marked in the order of P1–P10 cut from the seed end to the tail end. Fig. 1(b) shows these samples illuminated by a red LED, revealing minor scattering centers in the samples P1–P5 with the most severe in sample P3. Fig. 1(c) shows 10 samples C1–C10 cut from the

Manuscript received August 31, 2018; revised October 29, 2018; accepted November 30, 2018. Date of publication December 5, 2018; date of current version January 17, 2019. This work was supported in part by the U.S. Department of Energy, Office of High Energy Physics Program under Award DE-SC0011925, in part by the Fundamental Research Funds for the Central Universities of China, in part by the Natural Science Funds of Tianjin under Grant 18JCYBJC17800, and in part by the Natural Science Funds of China under Grant 51402332 and Grant 11775120.

F. Yang was with HEP, California Institute of Technology, Pasadena, CA 91125 USA. He is now with the Key Laboratory of Weak-Light Nonlinear Photonics, Ministry of Education, School of Physics, Nankai University, Tianjin 300071, China (e-mail: fan@nankai.edu.cn).

J. Chen was with HEP, California Institute of Technology, Pasadena, CA 91125 USA. He is now with the Key Laboratory of Transparent Opto-Functional Inorganic Materials, Shanghai Institute of Ceramics, Chinese Academy of Sciences, Shanghai 201899, China (e-mail: jfchen@mail.sic.ac.cn).

L. Zhang, C. Hu, and R.-Y. Zhu are with HEP, California Institute of Technology, Pasadena, CA 91125 USA (e-mail: zhu@hep.caltech.edu).

Color versions of one or more of the figures in this paper are available online at http://ieeexplore.ieee.org.

Digital Object Identifier 10.1109/TNS.2018.2884975

TABLE I
CONCENTRATIONS OF LANTHANUM, CERIUM, AND LEAD IN LA/CE CO-DOPED SAMPLES

| Sample ID. | Concentration (wt%) | | |
|---|---|---|---|
| | La | Ce | Pb |
| C1 | 2.015 | 0.0065 | <0.002 |
| C2 | 2.064 | 0.0069 | <0.002 |
| C3 | 2.299 | 0.0076 | <0.002 |
| C4 | 2.242 | 0.0075 | <0.002 |
| C5 | 1.953 | 0.0067 | <0.002 |
| C6 | 1.795 | 0.0060 | <0.002 |
| C7 | 1.379 | 0.0047 | <0.002 |
| C8 | 1.216 | 0.0043 | <0.002 |
| C9 | 1.147 | 0.0041 | <0.002 |
| C10 | 0.771 | 0.0029 | <0.002 |

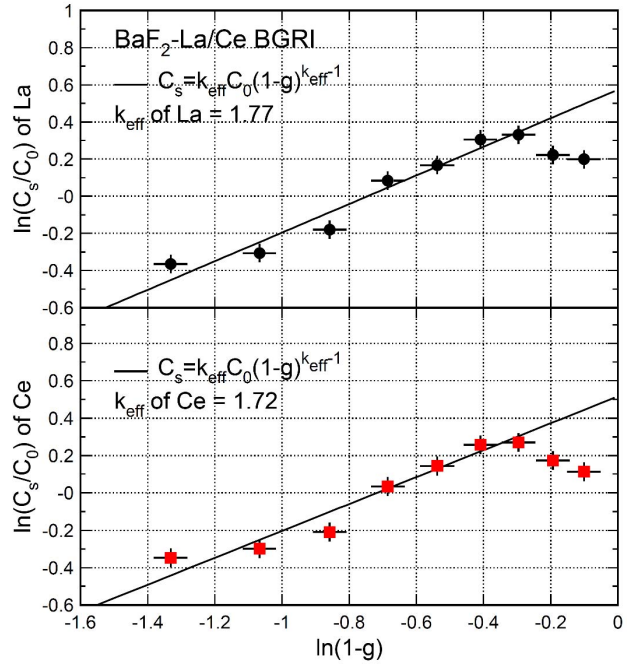


Fig. 2. Relative concentration of La (top) and Ce (bottom) as a function of solidification fraction in La/Ce co-doped $BaF_2$ samples.

adjacent positions of the samples P1–P10, respectively, from the same ingot for trace analysis.

Table I lists the trace concentration levels for La, Ce, and Pb determined by ICP-OES. The results show no Pb contamination and consistent distributions for La and Ce, where their trace concentration increases from C1 (seed end) to C3 and then decreases gradually from C3 to C10 (tail end). The shape of these distributions is consistent with the La distribution in the La-doped crystals grown by SIC discussed in the Part I of this paper. As discussed in the Part I of this paper, such distribution indicates an unstable crystallization velocity as explained by the BPS relation [11].

Similarly, we use data from the samples C3–C10 to extract effective segregation coefficients for La and Ce in $BaF_2$. Fig. 2 shows the fit results of $1.77 \pm 0.09$ and $1.72 \pm 0.09$, respectively, for La and Ce with a crystal growth velocity of 1.5 mm/h. The consistent effective segregation coefficients of La and Ce in $BaF_2$ are due to their similar ion radius and valance.

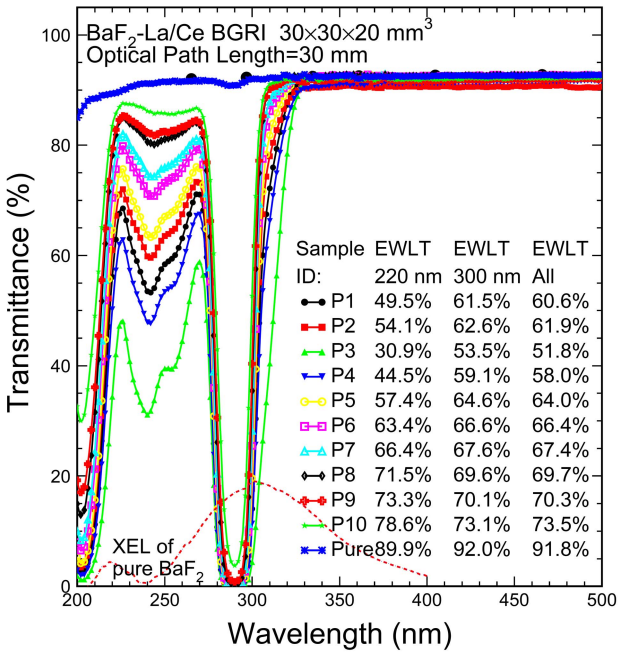


Fig. 3. Transmittance of 10 La/Ce co-doped $BaF_2$ crystal samples cut from the same ingot.

Fig. 3 shows transmission spectra of a pure and 10 La/Ce co-doped samples measured along 3-cm optical path length. Also shown in Fig. 3 are the EWLT values for the fast, slow and entire (all) emission. The transmittance of the samples P6–P10 approaches the theoretical limit (black dots) between 350 and 500 nm, indicating excellent optical quality. Three absorption bands peaked at 204, 240, and 290 nm are observed. The 240-nm absorption band is attributed to Ce-doping since it does not exist in the La-doped $BaF_2$. While the 204-nm absorption band is certainly due to La-doping, the 290-nm absorption band is also due to Ce-doping since it is located at the Ce absorption band in Ce-doped $BaF_2$ [6], [9], [12], [13].

The intensities of all three absorption bands are weakened from the seed end to the tail end because of the large segregation coefficients of La and Ce. The overlap between these absorption and emission bands in doped $BaF_2$ samples induces a self-absorption effect, which reduces scintillation light output. While the self-absorption effect induced by the 204-nm absorption band reduces the fast component, the self-absorption effect induced by the 240-nm absorption band reduces both fast and slow components. The self-absorption effect induced by the 290-nm absorption band reduces the slow component only, so improves the F/S ratio.

Fig. 4 shows correlations between the values of EWLT for the fast (220 nm, top left) and slow (300 nm, top right) scintillation components as well as their ratio (bottom) as a function of the La (left) and Ce (right) concentrations. The excellent linearity observed in two top plots indicates that the La/Ce concentration may be extracted from the EWLT data. The ratio distributions indicate that the optimized doping level for La and Ce is 0.77 and 0.0029 wt%, respectively, for slow component suppression in the La/Ce co-doped $BaF_2$.

In a brief summary, La and Ce dopings suppress the slow component and improve the F/S ratio. Some loss of the

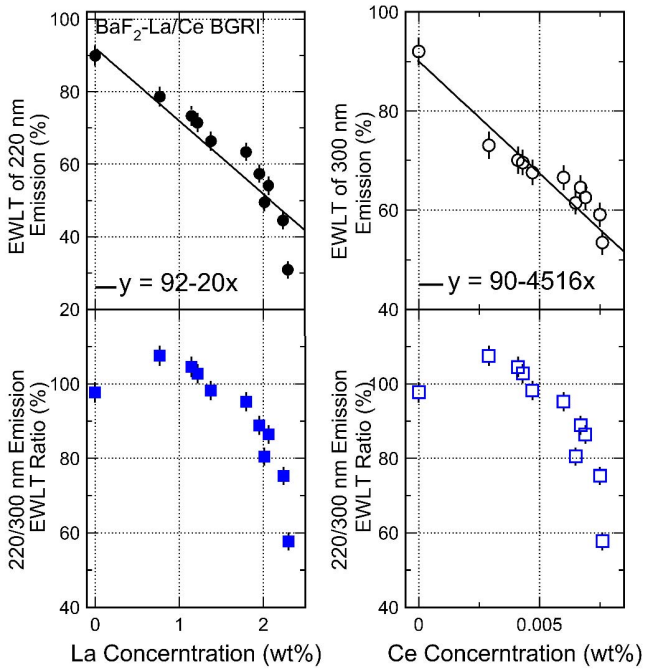


Fig. 4. Values of EWLT for the fast (220 nm, top left) and slow (300 nm, top right) scintillation components as well as their ratio (bottom) are shown as a function of the La (left) and Ce (right) concentrations.

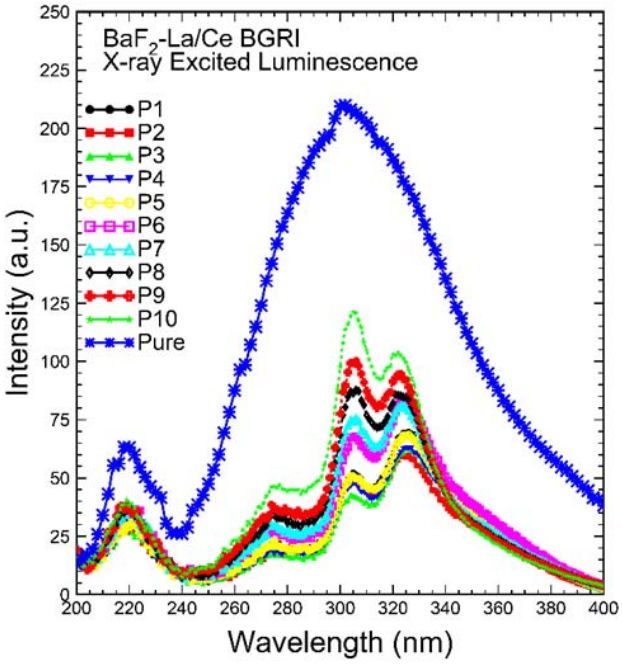


Fig. 5. Comparison of XEL spectra for pure and La/Ce co-doped $BaF_2$.

intensity for both the fast and slow components, however, is expected because of the absorption bands at 204 and 240 nm induced by the La and Ce-doping, respectively.

Fig. 5 shows the XEL spectra measured in the reflection mode for one pure and 10 La/Ce-doped $BaF_2$ crystals. There are four emission peaks at 220, 270, 305, and 325 nm observed in La/Ce co-doped $BaF_2$. While the 220-nm peak is consistent with the fast component in $BaF_2$, the other three emission peaks are dues to the overlap of the $Ce^{3+}$ luminescence peaks

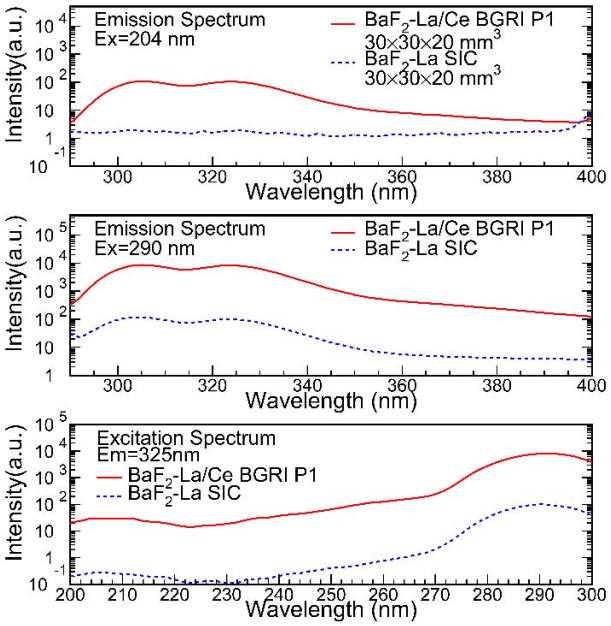


Fig. 6. Comparison of photo-luminescence spectra for a La/Ce co-doped and a La-doped $BaF_2$.

at 305 and 325 nm [9], [12], [13] with the slow component peaked at 300 nm.

The $Ce^{3+}$ luminescence may also be observed in the photo-luminescence (PL) spectrum. The top and middle plots of Fig. 6 show the PL spectra for a La/Ce co-doped and a La-doped $BaF_2$ samples excited by 204- and 290-nm light, respectively. Two emission bands peaked at 305 and 325 nm are observed in both samples, which are attributed to the 5d–4f electronic transitions of $Ce^{3+}$ in the $BaF_2$ crystal [9], [12], [13]. They are consistent with the XEL spectra shown in Fig. 5.

The PL intensity excited by 290-nm light in the La-doped $BaF_2$ sample is about two orders of magnitude lower than that in the La/Ce co-doped $BaF_2$ samples, indicating that the level of Ce contamination in the La-doped $BaF_2$ samples is about 1% of that in the La/Ce-doped samples or about 0.7 ppm, confirming that it is below the ICP-OES detection limit of 7 ppm. In addition, no PL is observed in the La-doped $BaF_2$ sample when excited by 204 nm, confirming that the Ce contamination in the La-doped $BaF_2$ sample is low.

Fig. 6 (bottom) shows the excitation spectra for the emission light at 325 nm. Two excitation bands peaked at 204 and 290 nm were observed. The relatively strong excitation band peaked at 290 nm corresponds to the 4f–5d transition of $Ce^{3+}$. The relatively weak excitation band peaked at 204 nm shows an intensity of three orders of the magnitude lower than that of 290-nm excitation band, indicating that the QE of the energy transfer between the 204-nm excitation band and the 325-nm emission is extremely low.

Fig. 7 shows the decay time of 25 ns measured by using the FLS920 fluorescence spectrophotometer with the time-correlated single photon counting technique when the PL and excitation wavelengths are fixed, respectively, at 324 and 291 nm for the La/Ce co-doped $BaF_2$ sample P1. The observed

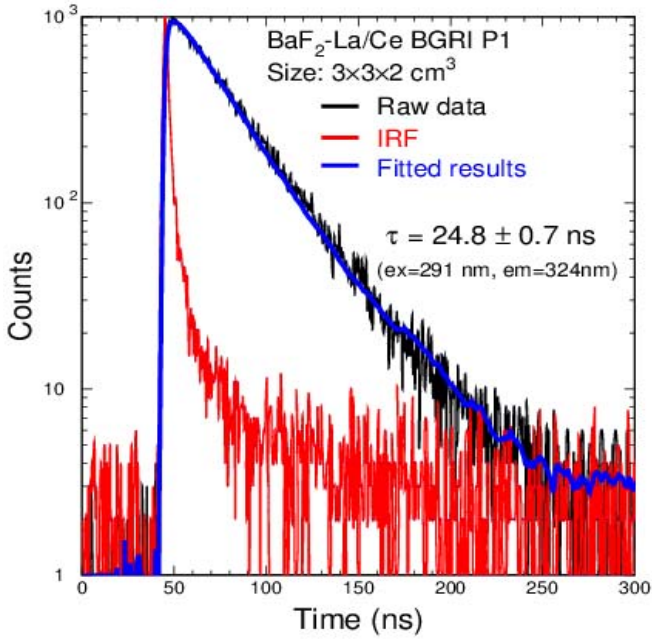


Fig. 7. Decay kinetics of PL of the La/Ce co-doped $BaF_2$ sample.

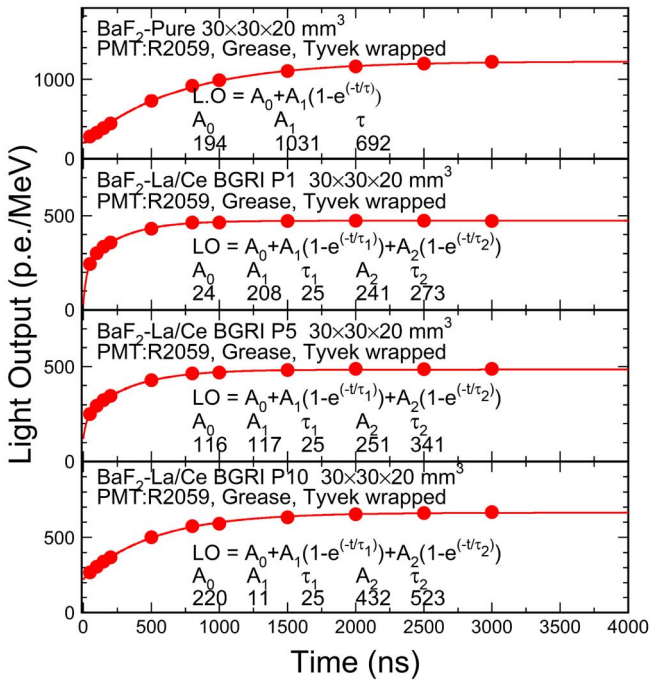


Fig. 8. Light output is shown as a function of the integration time for pure and La/Ce co-doped $BaF_2$ samples excited by $\gamma$-rays.

25-ns decay time is due to the $Ce^{3+}$ contribution to the luminescence in the La/Ce co-doped $BaF_2$ crystal.

Fig. 8 shows the light output as a function of the integration time for one pure and three La/Ce co-doped $BaF_2$ samples excited by a Na-22 source. To accommodate the Ce luminescence with 25-ns decay time, the measured data were fitted to two time constants, and a sub-nanosecond component $A_0$. Significant reductions are observed in both the light output and decay time of the slow component in the La/Ce co-doped $BaF_2$ samples, which is attributed to quenching centers

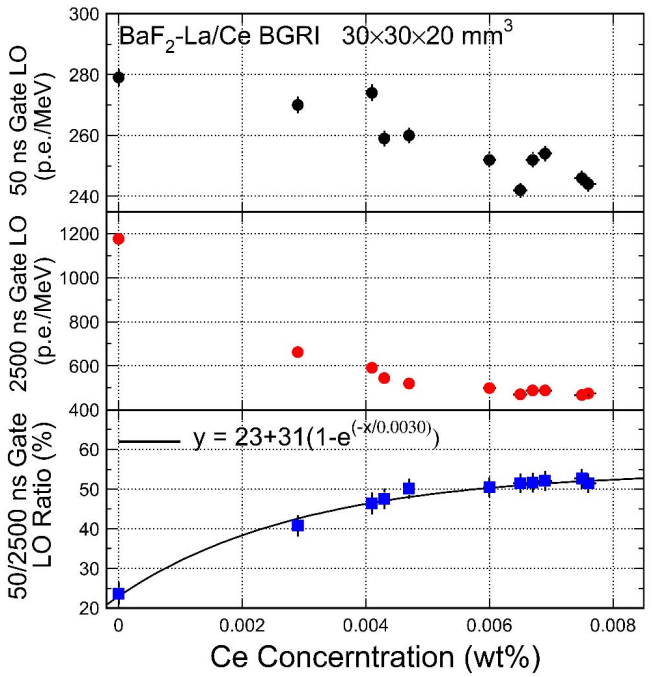


Fig. 9. Light output in 50- (top) and 2500-ns gate (middle) and their ratio are shown as a function of the Ce concentration in La/Ce co-doped $BaF_2$.

introduced by the La doping. In conclusion, the La/Ce co-doping suppresses the slow component and improves the F/S ratio.

Fig. 9 shows the light output in 50- (top) and 2500-ns gate (middle), and their ratio (bottom) as a function of the Ce concentration. While the light output in both 50- and 2500-ns gate decreases when the Ce concentration increases, their ratio increases. To maintain the light output of the fast component, the Ce concentration should be less than 0.005 wt% for an optimized F/T ratio.

Fig. 10 shows the light output in 50- (top) and 2500-ns gate (middle) and their ratio (bottom) as a function of the La concentration for La-doped (circles and squares) and La/Ce co-doped $BaF_2$ crystals (dots and cubes).

The light output in both 50- and 2500-ns gate in the La/Ce co-doped crystals is almost twice of that in the La-doped crystals for two reasons. First, the La/Ce co-doped crystals have a better overall optical quality. Second, the Ce doping introduces a combined effect of absorption and emission. The light output in both 50- and 2500-ns gate decreases linearly with the increased La concentration. To maintain the light output in 50-ns gate, the La concentration in the La/Ce co-doped crystals should also be less than 0.75 wt%.

Compared to the pure sample, a significant reduction of the slow component is observed in the La/Ce co-doped $BaF_2$ while the reduction of the fast component is much less. The bottom plot of Fig. 10 shows the F/T ratio increased from 1/6 to 1/2 for La/Ce co-doped samples, corresponds to the F/S ratio from 1/5 to 1/1, similar to La-doped samples reported in the Part I of this paper. The La/Ce co-doped samples in this investigation show a better light output of the fast component as compared to the Ce-doped samples reported

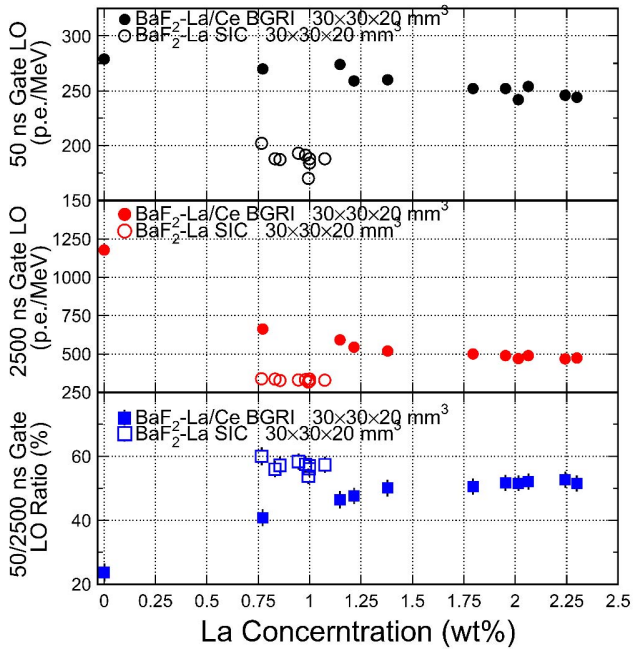


Fig. 10. Light output in 50- (top) and 2500-ns gate (middle) and their ratio (bottom) are shown as a function of the La concentration in both La-doped and La/Ce co-doped $BaF_2$ crystals.

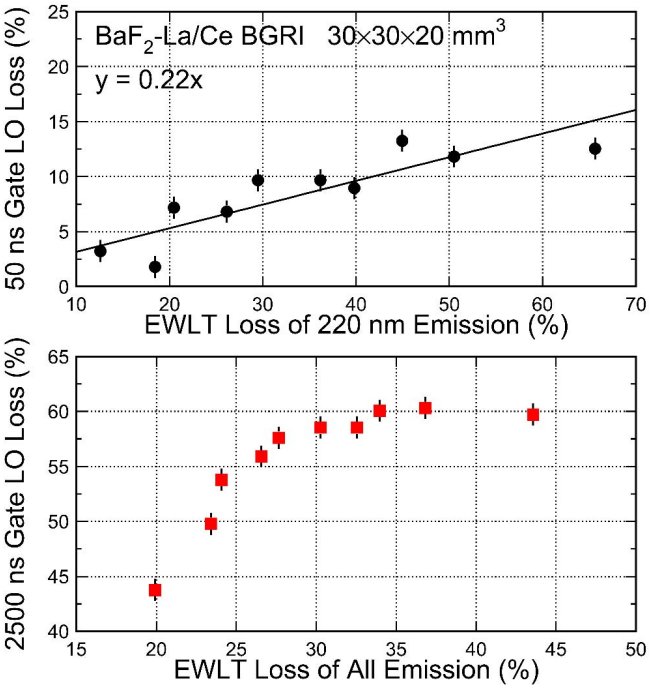


Fig. 11. Light output in 50- (top) and 2500-ns gate (bottom) is shown as a function the EWLT loss for La/Ce co-doped $BaF_2$.

by Yang *et al*. [6], Woody *et al.* [8], Dorenbos *et al*. [9], and Kurosawa *et al*. [10].

Fig. 11 shows the light output losses in 10 La/Ce co-doped $BaF_2$ samples compared to the pure sample in 50- (top) and 2500- (bottom) ns gate as a function of the EWLT loss. A good correlation is observed between the losses of the light output in 50-ns gate and the EWLT of the 220-nm emission, indicating that the loss of the fast scintillation


Fig. 12. 20-cm-long $BaF_2$ crystal co-doped with La and Ce.

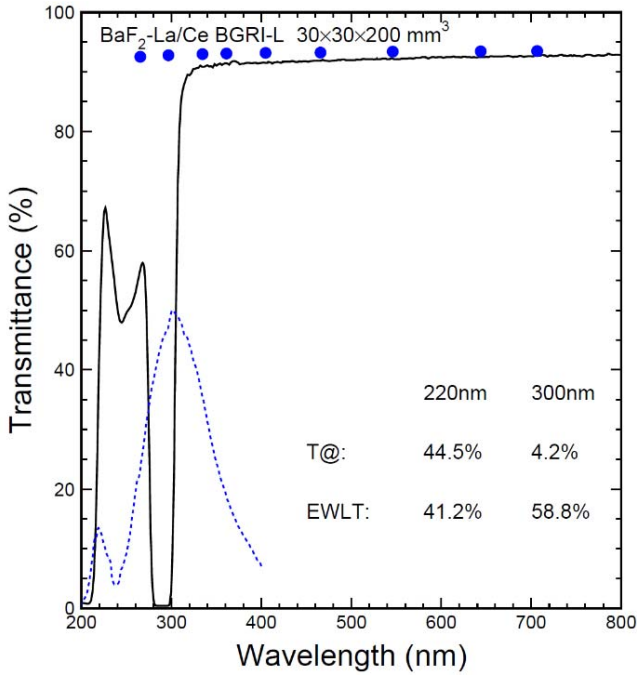


Fig. 13. Longitudinal transmittance of the 20-cm-long $BaF_2$ crystal co-doped with La and Ce.

component is due to the absorption induced by La doping. No correlation is observed between the losses of the light output in 2500-ns gate and the EWLT for the entire emission, indicating an additional quenching effect beyond absorption, which is discussed in the Part I of this paper.

Together with the 20 small La/Ce co-doped $BaF_2$ samples, a 20-cm-long sample was also cut from the same ingot at BGRI. Fig. 12 shows photograph of a La/Ce co-doped $BaF_2$ crystal of $3 \times 3 \times 20$ $cm^3$. Fig. 13 shows its longitudinal transmission spectrum, which approaches the theoretical limit between 350 and 800 nm, indicating its excellent optical quality free of scattering centers. Absorption bands are observed around 204, 240, and 290 nm, which are due to the La/Ce co-doping. These bands are consistent with the transmission spectra observed in Fig. 3 for small samples.

Fig. 14 shows the transverse transmission spectra measured at seven points evenly distributed along the 20-cm-long axis of the sample. The optical path length in the transmittance measurement is 3 cm, which is identical to that of the 10 small samples shown in Fig. 3. The intensity of the three absorption bands around 204, 240, and 290 nm weakens from the seed end to the tail end because of the segregation of La and Ce in $BaF_2$. According to the relations between the EWLT and the concentrations of La and Ce shown in Fig. 4, the La and Ce concentrations may be extracted to be from 1.1 to 0.7 wt%

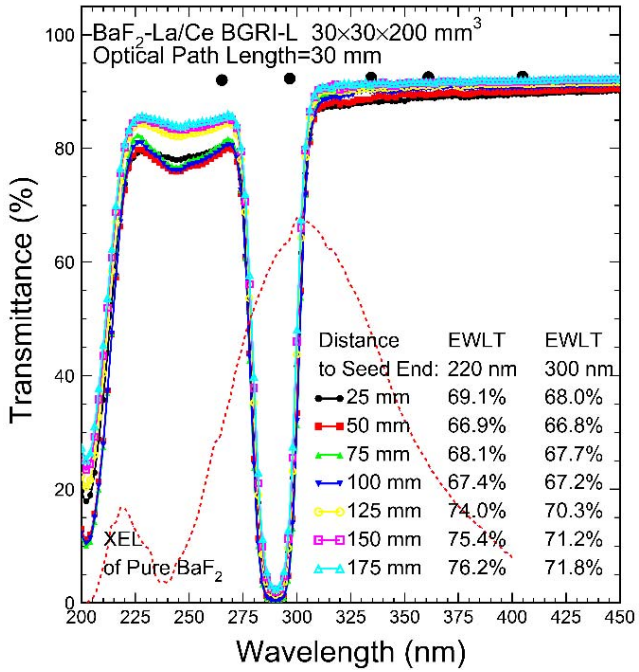


Fig. 14. Transverse transmittance measured along 3-cm light path for the 20-cm-long $BaF_2$ crystal co-doped with La and Ce.

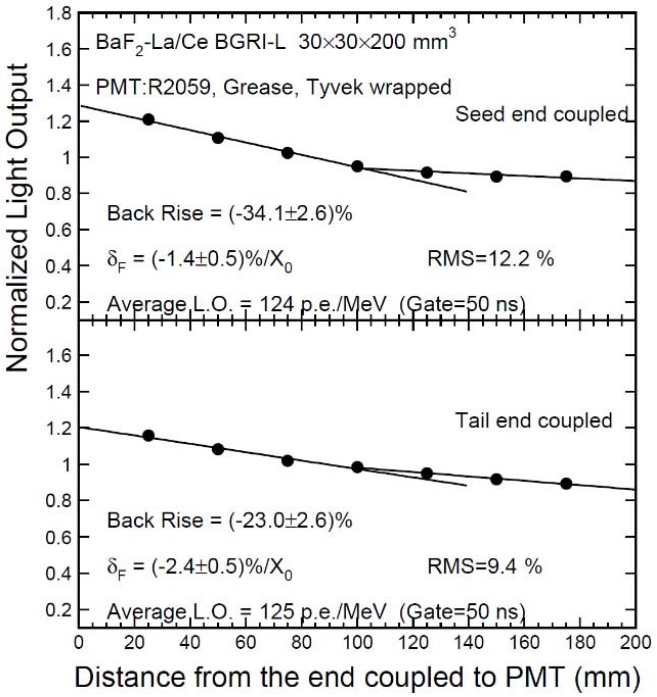


Fig. 15. Light output is shown as a function of the distance to the photodetector for the 20-cm-long La/Ce co-doped $BaF_2$ crystal.

and 0.0049 to 0.0040 wt% from seed to tail, respectively. The variation of La and Ce concentrations of this large sample is relatively smaller than that of 10 small samples, which is probably due to a lower crystal growth velocity for the large sample at BGRI.

Fig. 15 shows light output of 50-ns gate as a function of distance to the photodetector for this 20-cm-long La/Ce co-doped $BaF_2$ crystal with the seed (top) and tail (bottom) end coupled to the PMT. This 20-cm-long doped $BaF_2$ crystal has a similar light response uniformity as compared to the pure $BaF_2$ crystal of the same size [6], indicating that this doping approach is promising for future HEP applications. The overall F/T ratio, however, was found increased from 1/6 to 1/2 as compared to undoped $BaF_2$ crystals, corresponding to an F/S ratio from 1/5 to 1/1. The F/S ratio at this level alone is judged to be not sufficient for mitigating the pile-up effect, so additional slow suppression by using solar-blind photodetector would be required.

## III. Conclusion

The ultrafast scintillation light with sub-nanosecond decay time in $BaF_2$ crystals provides sufficient light for an ultrafast calorimeter. The issue of $BaF_2$ crystal's slow scintillation light with 600-ns decay time can be handled by several approaches: selective doping, selective readout with solar blind photodetector, and heating the crystal.

La/Ce co-doped $BaF_2$ crystals were grown at BGRI and investigated at Caltech. The La/Ce co-doped $BaF_2$ crystals grown at BGRI have good optical quality with the effective segregation coefficients of $1.77 \pm 0.09$ and $1.72 \pm 0.09$, respectively, for La and Ce in $BaF_2$ with a crystal growth velocity of 1.5 mm/h.

Both the La and Ce-doping in the $BaF_2$ reduce light output of the slow component more than the fast component. The slow suppression of the La/Ce co-doping is due to both quenching for its STE light and absorption from $Ce^{3+}$ where the later also generates scintillation light of 25-ns decay time. A 20-cm-long La/Ce co-doped $BaF_2$ crystal grown at BGRI shows excellent optical quality and a promising performance in the light response uniformity.

Consequently, both La and La/Ce-doping improve the F/S ratio from about 1/5 to better than 1/1, which, however, is judged to be not sufficient to mitigate the pile-up effect.

Our previous investigation shows that both BGRI and SIC provided large-size undoped $BaF_2$ crystals of good quality for the Mu2e experiment [14]. Both manufactures, however, encounter similar issues in developing rare earth-doped $BaF_2$ crystals of large size. While BGRI successfully grew a large-size La/Ce co-doped $BaF_2$ of good optical quality and optimized the yttrium doping level in $BaF_2$ crystals of small size [15], SIC has successfully grown the first yttrium-doped $BaF_2$ crystal of large size [16].

Recently, we found that Y doping is more effectively in suppressing the slow component in $BaF_2$ crystals as suggested in the early investigation for mixed powders [17]. An F/T ratio up to 80% was observed in small samples while the fast component remains unchanged [15], [16], which is significantly more effective than the data published in this investigation. Our plan is to continue yttrium doping for future ultrafast HEP calorimeters at the energy and intensity frontiers. Research and development along this direction has been continued with yttrium doping.

## Acknowledgment

The authors would like to thank the Mu2e collaboration for providing the $BaF_2$ samples discussed in this paper as well as many useful discussions.

## REFERENCES


[1] R. Novotny, "The $BaF_2$ photon spectrometer TAPS," *IEEE Trans. Nucl. Sci.*, vol. 38, no. 2, pp. 379–385, Apr. 1991.

[2] R. Y. Zhu, "Signal and background of H→ $\gamma\gamma$ with proposed GEM calorimeter systems," Fermilab, Batavia, IL, USA, Tech. Rep. GEM TN-91-32 and CALT 68-1777, Nov. 1991.

[3] R. Y. Zhu and H. Yamammoto, "Intermediate mass higgs searches with the GEM detector," Fermilab, Batavia, IL, USA, Tech. Rep. GEM TN-91-32 and CALT 68-1777, Jul. 1992.

[4] S. Mrenna, S. Shevchenko, X. R. Shi, H. Yamamoto, and R. Y. Zhu, "GEM TN-93-373 and CALT 68-1856," Tech. Rep., 1993.

[5] G. Pezzulloin *et al.*, "The LYSO crystal calorimeter for the Mu2e experiment," *J. Instrum.*, vol. 9, no. 3, p. C03018, 2014.

[6] F. Yang, J. Chen, L. Zhang, and R. Zhu, "Development of $BaF_2$ crystals for future HEP experiments at the intensity frontiers," in *Proc. IEEE Nucl. Sci. Symp., Med. Imag. Conf. Room-Temp. Semiconductor Detector Workshop (NSS/MIC/RTSD)*, Oct. 2016, pp. 1–4.

[7] R. Visser, P. Dorenbos, C. W. E. van Eijk, R. W. Hollander, and P. Schotanus, "Scintillation properties of $Ce^{3+}$ doped $BaF_2$ crystals," *IEEE Trans. Nucl. Sci.*, vol. 38, no. 2, pp. 178–183, Apr. 1991.

[8] C. L. Woody, P. W. Levy, and J. A. Kierstead, "Slow component suppression and radiation damage in doped $BaF_2$ crystals," *IEEE Trans. Nucl. Sci.*, vol. 36, no. 1, pp. 536–542, Feb. 1989.

[9] P. Dorenbos, R. Visser, R. W. Hollander, C. W. E. Van Eijk, and H. W. Den Hartog, "The effects of $La^{3+}$ and $Ce^{3+}$ dopants on the scintillation properties of $BaF_2$ crystals," *Radiat. Effects Defect Solids*, vols. 119–121, pp. 87–92, Nov. 1991.

[10] S. Kurosawa, T. Yanagida, Y. Yokota, and A. Yoshikawa, "Crystal growth and scintillation properties of fluoride scintillators," *IEEE Trans. Nucl. Sci.*, vol. 59, no. 5, pp. 2173–2176, Oct. 2012.

[11] J. A. Burton, R. C. Prim, and W. P. Slichter, "The distribution of solute in crystals grown from the melt. Part I. Theoretical," *J. Chem. Phys.*, vol. 21, no. 11, pp. 1987–1991, 1953.

[12] V. Nesterkina, N. Shiran, A. Gektin, K. Shimamura, and E. Villora, "The Lu-doping effect on the emission and the coloration of pure and Ce-doped $BaF_2$ crystals," *Radiat. Meas.*, vol. 42, pp. 819–822, Apr. 2007.

[13] W. Drozdowski, K. R. Przegietka, A. J. Wojtowicz, and H. L. Oczkowski, "Charge traps in Ce-doped $CaF_2$ and $BaF_2$," *Acta Phys. Polym. A*, vol. 95, pp. 251–258, Feb. 1999.

[14] R. Y. Zhu, "Calorimeter technical review: Crystals: Quality & radiation hardness Mu2e CTR review," to be published.

[15] R.-Y. Zhu, "Very fast inorganic crystal scintillators," *Proc. SPIE*, vol. 10392, p. 103920G, Sep. 2017.

[16] J. Chen, F. Yang, L. Zhang, R.-Y. Zhu, Y. Du, and S. Wang, "Slow scintillation suppression in yttrium doped $BaF_2$ crystals," *IEEE Trans. Nucl. Sci.*, vol. 65, no. 8, pp. 2147–2151, Aug. 2018.

[17] B. P. Sobolev, E. A. Krivandina, S. E. Derenzo, W. W. Moses, and A. C. West, "Suppression of $BaF_2$ slow component of X-RAY luminescence in non-stoichiometric $Ba_{0.9}R_{0.1}F_{2.1}$ crystals (R=Rare Earth Element)," *Proc. Mater. Res. Soc., Scintillator Phosphor Mater.*, vol. 348, pp. 277–283, Feb. 1994.